Springer

Journal of Mechanical Science and Technology 23 (2009) 1743~1750

Journal of Mechanical Science and Technology

www.springerlink.com/content/1738-494x
DOI 10.1007/s12206-009-0410-8

Analysis of flame shapes in turbulent hydrogen jet flames with coaxial air †

Hee-Jang Moon*

School of Aerospace and Mechanical Engineering, Korea Aerospace University, 200-1 Hwajeon-dong, Duckyang-gu, Koyang-shi, Kyungki-do 412-791, Korea

(Manuscript Received February 26, 2008; Revised March 16, 2009; Accepted March 19, 2009)

Abstract

This paper addresses the characteristics of flame shapes and flame length in three types of coaxial air flames realizable by varying coaxial air and/or fuel velocity. Forcing coaxial air into turbulent jet flames induces substantial changes in flame shapes and NOx emissions through the complex flow interferences that exist within the mixing region. Mixing enhancement driven by coaxial air results in flame volume decrease, and such a diminished flame volume finally reduces NOx emissions significantly by decreasing NOx formation zone where a fuel/air mixture burns. It is found that mixing in the vicinity of high temperature zone mainly results from the increase of diffusive flux than the convective flux, and that the increase of mass diffusion is amplified as coaxial air is increased. Besides, it is reaffirmed that non-equilibrium chemistry including HO_2/H_2O_2 should be taken into account for NOx prediction and scaling analysis by comparing turbulent combustion models. In addition, it is found that coaxial air can break down the self-similarity law of flames by changing mixing mechanism, and that EINOx scaling parameters based on the self-similarity law of simple jet flames may not be eligible in coaxial air flames.

Keywords: Coaxial jet; EINOx; Flame length; Nonpremixed flame; Turbulent flow

1. Introduction

To clarify the characteristics of NOx formation in turbulent nonpremixed hydrogen-air jet flames, Driscoll et al. [1, 2] conducted a series of experiments in which the effects of radiation, buoyancy, and coflow air were minimized. They found 1/2-power scaling between EINOx (emission index of NOx, NOx[g]/Fuel[kg]) normalized by flame residence time and global strain rate, and attributed the observed tendency to variations in flame thickness in response to the change of flame Damköhler number. Chen and Kollmann [3] showed that such EINOx scaling is due to nonequilibrium effect. In analyzing the influences of different reduced chemical models on EINOx scaling, Chen et al. [4] found that the 1/2-power scaling could be reproduced using a detailed chemical model. Schlatter et al. [5] explained via PEUL (Probabilistic EUlerian Lagrangian) model that the 1/2-power scaling results from different radical concentration levels controlled by the slow recombination reactions. Sanders et al. [6] and Schlatter et al. [5] analyzed NOx formation by laminar flamelet model, but failed to reproduce the 1/2-power scaling. These previous NOx studies on turbulent nonpremixed hydrogen flames have focused on simple jet flames without coaxial air.

However, recent studies [7, 17] show that the EINOx scaling deviates from the 1/2 slope, and power scaling law [2] of turbulent diffusion flame without coaxial air may not be valid in the presence of coaxial air. The interest in turbulent nonpremixed flames with coaxial air is increasing these days, because high-

† This paper was recommended for publication in revised form by Associate Editor Haecheon Choi

*Corresponding author. Tel.: +82 2 300 0118, Fax.: +82 2 3158 3189
E-mail address: hjm@kau.ac.kr

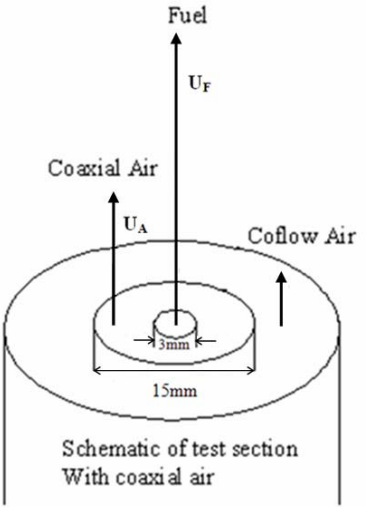

Fig. 1. Schematic of coaxial air jet (the coaxial air between fuel and coflow stream is usually injected faster than coflow air, U_A: coaxial air velocity; U_F: fuel velocity).

speed coaxial air is used in many practical combustive devices to enhance fuel/air mixing and further can be utilized as NOx reduction technology. It has been known that coaxial air can reduce the amount of entrained air required to dilute the fuel to stoichiometric proportions [2]. Therefore, the coaxial air between fuel and coflow stream is usually injected faster than coflow air, as sketched in Fig. 1. It is believed that coaxial air causes a variation of flame shapes, and indirectly leads to high reduction of NOx emissions. Driscoll et al. [1, 2] explained the large reduction by the fact that coaxial air reduces the flame length and thus decreases the local residence time as well as the reaction zone volume. Recently, in order to improve the understanding of the physical mechanisms associated with EINOx scaling in coaxial air flames, Kim et al. [7] conducted various experiments in hydrogen nonpremixed flames with coaxial air, varying either coaxial air or fuel velocity, or both.

They observed through a comparison of undiluted with He-diluted coaxial air flames that some deviations of EINOx scaling from 1/2-power may be due to difference of the radiation effect, because the amount of radiative heat loss that depends on the flame volume is altered by coaxial air. Besides radiation, flame length (i.e., flame volume) and nonequilibrium chemistry associated with NOx formation, the effect of flow dynamics such as convective and diffusive mixing process on NOx formation has not been studied in detail in coaxial flame. Therefore, a thorough emphasis will be given in this study to find the dominant controlling parameters of flow dynamics affecting NOx formation in coaxial flame. The specific objectives of the present study are: (1) to investigate the correlation existing between flow convection and mass diffusion on NOx formation, and (2) to clarify the changes of flame shapes and violation of flame self-similarity law. For these purposes, two classical turbulent combustion models that account for turbulence-chemistry interaction were used: the Lagrangian IEM (interaction by exchange with the mean) and the presumed joint PDF model. For chemistry, the partial equilibrium assumption was applied to consider nonequilibrium effect known to be a significant factor that affects 1/2-power scaling [3, 4]. We first calculated simple jet flames of Driscoll et al. [1, 2] in order to evaluate the applicability of present numerical schemes and models for NOx prediction, and then simulated various cases of coaxial air flames of Kim et al. [7]. In the next section, we will briefly describe the applied numerical methodologies and conditions, and then discuss our findings of coaxial air flames.

2. Governing equations and numerical models

The following fully coupled form of Favre averaged Navier-Stokes and $k-\varepsilon$ turbulent equations is used around axisymmetric geometry and solved with preconditioning method:

$$\Gamma\frac{\partial \mathbf{Q}_v}{\partial t}+\frac{\partial \mathbf{E}}{\partial x}+\frac{\partial \mathbf{F}}{\partial y}+\mathbf{H}=\frac{\partial \mathbf{E}_v}{\partial x}+\frac{\partial \mathbf{F}_v}{\partial y}+\mathbf{H}_v+\mathbf{W} \quad (1)$$

$$Q_v=\begin{bmatrix} p \\ u \\ v \\ T \\ k \\ \varepsilon \\ g \\ Y_{N_2} \\ Y^*_{H_2} \end{bmatrix} \Gamma=\begin{bmatrix} 1/\varepsilon_p c^2 & 0 & 0 & 0 & 0 & 0 & 0 & 0 & 0 \\ u/\varepsilon_p c^2 & \rho & 0 & 0 & 0 & 0 & 0 & 0 & 0 \\ v/\varepsilon_p c^2 & 0 & \rho & 0 & 0 & 0 & 0 & 0 & 0 \\ H/\varepsilon_p c^2-1 & \rho u & \rho v & \rho C_p & \frac{5}{3}\rho & 0 & 0 & 0 & 0 \\ k/\varepsilon_p c^2 & 0 & 0 & 0 & \rho & 0 & 0 & 0 & 0 \\ \varepsilon/\varepsilon_p c^2 & 0 & 0 & 0 & 0 & \rho & 0 & 0 & 0 \\ g/\varepsilon_p c^2 & 0 & 0 & 0 & 0 & 0 & \rho & 0 & 0 \\ Y_{N_2}/\varepsilon_p c^2 & 0 & 0 & 0 & 0 & 0 & 0 & \rho & 0 \\ Y^*_{H_2}/\varepsilon_p c^2 & 0 & 0 & 0 & 0 & 0 & 0 & 0 & \rho \end{bmatrix} \quad (2)$$

where Q_v is the vector of nonconservative variables and the preconditioning matrix Γ suggested by Choi and Merkle [8] is adopted. Here k and ε correspond to mean turbulence kinetic energy and dissipation rate, respectively, and g and Y_i represent the variance of mixture fraction and the mass fraction of the i^{th} spe-

cies. Two-dimensional axisymmetric flow is adopted with x being the axial and y the radial coordinates, respectively. The preconditioning parameter ε_P to control the stiffness of eigenvalues at low Mach number was determined as

$$\varepsilon_p = Min\left(1, Max\left(10^{-10}, M^2\right)\right) \tag{3}$$

2.1 Chemistry and radiation models

Two chemical models of Warnatz et al. [9] were applied: 7 species and 9 elementary reaction steps, 9 species and 19 elementary reaction steps. Based on the partial equilibrium assumption that fast shuffle reactions are assumed to be in equilibrium, Dixon-Lewis et al. [10] reduced the full chemical mechanism to a one-step global reaction. The combined variable Y^*_{H2} in the chemical model including HO_2/H_2O_2 chemistry was expressed by Louis [11] as follows:

$$\begin{aligned} Y^*_{H_2} = Y_{H_2} + \frac{M_{H_2}}{M_O}Y_O + \frac{3}{2}\frac{M_{H_2}}{M_H}Y_H + \frac{1}{2}\frac{M_{H_2}}{M_{OH}}Y_{OH} \\ - \frac{1}{2}\frac{M_{H_2}}{M_{HO_2}}Y_{HO_2} - \frac{M_{H_2}}{M_{H_2O_2}}Y_{H_2O_2} \end{aligned} \tag{4}$$

The source term for the combined variable Y^*_{H2} is derived as the summation of relatively linear source terms of third-body recombination reactions as follows:

$$\dot{\omega}^*_{H_2} = -2M_{H_2}(\dot{\omega}_5 + \dot{\omega}_6 + \dot{\omega}_7 + \dot{\omega}_8 + \dot{\omega}_{15}) \tag{5}$$

where $\dot{\omega}_i$ means the reaction rate of the i^{th} reaction step. Radicals O, H, and OH are determined by the partial equilibrium assumption and radicals HO_2 and H_2O_2 are obtained by the steady-state assumption.

For thermal NOx formation, the steady state assumption for the radical N is used. With $[NO]/[NO]_{eq} << 1$, the source term of NO from the extended Zeldovich mechanism can be approximated as

$$\dot{\omega}_{NO} = M_{NO}(2K_{f9}[N_2][O]) \tag{6}$$

where $K_{f9} = 1.84\times10^{14}\exp(-38370/T)\ cm^3/mol\cdot s$ and symbol [ ] denotes concentration.

As the radiative heat loss is known to be important in the prediction of NOx in jet flames without dilution, the optically thin assumption is applied. The radiation heat loss per unit volume can be expressed as

$$\Phi(T, p_{H_2O}) = 4\sigma p_{H_2O}K_{p,H_2O}(T^4 - T_b^4) \tag{7}$$

where the Planck mean absorption coefficient $K_{P,H2O}$ is calculated from the curve fit in the literature [12].

2.2 Turbulent combustion models

Two classical turbulent combustion models (Presumed PDF and Lagrangian models based on IEM) are applied to account for the turbulence-chemistry interaction. In the presumed joint PDF model, the state of reaction is determined by three nondimensionalized variables: mixture fraction, reaction progress variable, and normalized temperature.

$$\tilde{f} = \frac{\tilde{Z} - \tilde{Z}^a}{\tilde{Z}^f - \tilde{Z}^a} \tag{8}$$

$$\tilde{r} = \frac{\tilde{Y}^*_{H_2} - \tilde{Y}^{*\ u}_{H_2}}{\tilde{Y}^{*\ e}_{H_2} - \tilde{Y}^{*\ u}_{H_2}} = \frac{\tilde{Y}^*_{H_2} - \tilde{Y}^{*\ u}_{H_2}}{U(\tilde{f})} \tag{9}$$

$$\tilde{T}^* = \frac{\tilde{T} - \tilde{T}^{\min}}{\tilde{T}^{ad} - \tilde{T}^{\min}} = \frac{\tilde{T} - \tilde{T}^{\min}}{W(\tilde{f}, \tilde{r})} \tag{10}$$

where superscripts, 'e', 'u', and 'ad', indicate equilibrium, unburned, and adiabatic states, respectively. The mean properties which are not directly calculated by transport equations are interpolated from a Look-up Table.

If the fluctuations of nondimensionalized variables are assumed as being statistically independent of one another, the joint PDF can be simplified as the product of each PDF of nondimensionalized variables, and then, density-weighted averages are obtained by the following equation:

$$\tilde{\phi} = \iiint \phi(f, r, T^*)\tilde{P}(f)\tilde{P}(r)\tilde{P}(T^*)dfdrdT^* \tag{11}$$

The PDF for the mixture fraction is assumed to be the beta function, whereas the PDF's of the reaction progress variable and normalized temperature are assumed to be the delta function.

The second model which couples the Eulerian transport equations to the Lagrangian approach is based on IEM model introduced by Villermaux[13]. The Lagrangian equation governing the behavior of a fluid particle is modeled as

$$\frac{d\phi_i}{dt} = \frac{\tilde{\phi}_i - \phi_i}{\tau_{ex}} + \dot{\omega} \quad , \quad \phi_i = f, Y_i, h \tag{12}$$

where τ_{ex}, the turbulent mixing exchange time is given as $\tau_{ex} = C_t k/\varepsilon$ with $C_t = 1$.

The reaction and radiation source terms are de-

scribed as

$$\tilde{\dot{\omega}} = \iiint \dot{\omega}(f, Y_i, h)\tilde{P}(f, Y_i, h)dfdY_i dh$$
$$= \int \dot{\omega}(f, Y_i, h)\tilde{P}(Y_i \mid f)\tilde{P}(h \mid f)\tilde{P}(f)df \quad (13)$$

3. Results and discussion

3.1 Simple nonpremixed hydrogen jet flames

To investigate whether numerical models used in this study can capture the 1/2-power scaling ($EINOx/\tau_R = (U_F/D_F)^{1/2}$) when applied to simple jet flames, some experimental cases of Driscoll et al.[1,2] were first simulated. The inner diameters of fuel nozzles are 1.6, 2.6, and 3.7mm, and coflow air velocity is fixed at 0.5m/s for all the cases considered. Grid density of 141 by 98 was selected from the grid dependency test. Three different Models (models A, B and C) classified by the types of the combination of turbulent combustion models and chemical models were employed: Model A (presumed joint PDF and chemical model neglecting HO_2/H_2O_2), Model B (IEM and chemical model neglecting HO_2/H_2O_2), and Model C (presumed joint PDF and chemical model including HO_2/H_2O_2).

Fig. 2 represents the comparison of measured with predicted scalings between EINOx normalized by flame residence time ($EINOx/(L_f^3/U_F D_F^2)$) and global strain rate (U_F/D_F). While Models A and B overestimate EINOx and produce higher slopes of 0.8 to 0.9, Model C not only predicts EINOx to an acceptable level, except in the region of the low global strain rate ($U_F/D_F<10^5$), but also follows 1/2 slope which is almost consistent with experimental results. Models A, B, and C all show slightly higher slopes in the region of the low global strain rate. Chen and Kollmann [3] attributed this tendency to the overestimated radiative heat loss due to the incompleteness of the radiation model. The influence of the turbulent combustion models on NOx emissions can be investigated by comparing Model A to Model B in Fig. 2. Although the IEM model overpredicts EINOx more than the presumed joint PDF model, both models produce almost the same tendency of NOx scaling.

It is noted that Model C including HO_2/H_2O_2 chemistry not only reproduces 1/2-power scaling, but also predicts EINOx most correctly among the three Models in the region of the high global strain rate. It is known that HO_2/H_2O_2 chemistry tends to prevent the overestimation of EINOx, enhancing the decay

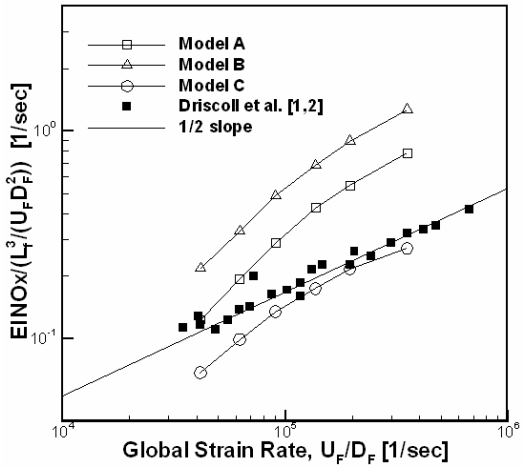

Fig. 2. Comparisons of predicted and measured EINOx scaling in simple nonpremixed jet flames of Driscoll et al. [1, 2].

rate of radical pool by providing extra third-body recombination paths [11]. The overestimation of nonequilibrium effect typically overpredicts NOx, because the increase of NOx through superequilibrium O-radical exceeds its decrease through subequilibrium temperature. Therefore, the correct consideration of nonequilibrium effect using an appropriate chemical model is imperative in the prediction of EINOx and its scaling. This sensitivity of NOx formation to nonequilibrium effect supports the fact that EINOx scaling depends on Damköhler number [1,2,3]. Hereafter, Model C is used for the remainder of the numerical calculations since it shows the best concordance with the experiments' data among the three models.

3.2 Nonpremixed hydrogen jet flames with coaxial air

Physical effects that affect NOx formation in turbulent hydrogen jet flames are nonequilibrium chemistry, radiation effect, and flow dynamics when coflow and buoyancy effects are suppressed. In the preceding results, we reaffirmed that nonequilibrium chemistry may be one of the cause of EINOx 1/2-power scaling in simple jet flames. For the radiation effect, though it has an important role in NOx reduction, its effect is beyond the scope of this work. The last important factor, flow dynamics, can make a significant difference in NOx emissions by changing fuel/air mixing. That is, mixing which is intensified by the shear force triggered from the coaxial jet can play a vital role in NOx formation. Since thermal NOx emissions are

strongly related to NOx formation zone where temperature is over 1800K, it is evident that mixing enhancement of local hot spots will cause NOx reduction by decreasing NOx formation zone. This implies that the coaxial air velocity can be used as a major parameter for controlling NOx emissions by changing fuel/air mixing strength.

A numerical analysis for various experiments of Kim et al. [7] was conducted. The inner diameter and the lip thickness of the fuel nozzle are 3.0mm and 0.5mm, respectively. The coaxial air nozzle has a diameter of 15mm and is concentric to the fuel nozzle. Experimental conditions are classified into three categories according to the variations of fuel and coaxial air velocities: Case I (increasing U_F, with U_A fixed at 10 or 20m/s), Case II (increasing both U_F and U_A, with U_A/U_F fixed at 0.051 or 0.068), Case III (increasing U_A, with U_F fixed at 140 or 244m/s). The detailed numerical conditions are tabulated in Table 1. Coflow air velocity and initial temperature are fixed at 1m/s and 298K, respectively. Here, Model C that shows the best results in the calculation of simple jet flames is used.

Fig. 3 represents the comparison of predicted with measured flame lengths for all the cases. Good agreement with experimental results is shown in the region of the low U_A/U_F, which is close to simple jet flames. These agreements are because model constant $C_{\varepsilon 1}$ in the production term of $k-\varepsilon$ model is modified to 1.48 so that the flame length can be predicted quite accurately in the calculation of simple jet flames of Barlow and Carter [14]. However, as the ratio of coaxial air to fuel velocity rises, notable differences from experimental results are found in the region of the high U_A/U_F. This overestimation of a flame length implicates that $k-\varepsilon$ model adjusted to simple jet flames does not account for the effect of coaxial air on turbulent flows. The single trimming method used in this study for the $k-\varepsilon$ model can be, however, qualified because we confirmed that the standard $k-\varepsilon$ model and Pope [15] correction lead to the same conclusion on flame shape and EINOx scaling. Besides, these errors of flame length are not a matter that can be corrected solely by the exact use of model, because it is sensitive to turbulent Schmidt number as well.

Table 1. Numerical conditions in the present study, Case I: fixed U_A=10, 20m/s, Case II: fixed U_A/U_F=0.051, 0.068, Case III: fixed U_F=140, 244m/s (fixed values are in bold letter).

	U_F (m/s)	U_A (m/s)	U_A/U_F
Case I	150~470	**10.0**	0.021~0.066
	160~470	**20.0**	0.042~0.125
Case II	140~380	9.52~25.8	**0.068**
	140~390	7.14~19.9	**0.051**
Case III	**140**	3~25	0.021~0.178
	244	3~25	0.012~0.102

Fig. 3 also shows that the length of coaxial air flames decreases as the ratio of coaxial air to fuel velocity increases. This behavior accords with the literature of Dahm and Mayman [16] and of Driscoll et al. [2]. According to them, coaxial air reduces the flame length by decreasing the amount of coflow air required to dilute the fuel to stoichiometric ratio. The causes of such flame reduction due to mixing enhancement are worth analyzing by a more thorough investigation.

3.3 Effect of convective and diffusive flux

In the present study, two dominant mixing processes, flow convection and mass diffusion, are separately analyzed to illustrate mixing mechanisms triggered by coaxial air. Convective and diffusive mass fluxes of oxygen Y_{O2} passing through the stoichiometric surface, are chosen as parameters to quantify the effects of coaxial air on two mixing processes. They are defined as:

$$\dot{m}_{O_2,CONV} = \delta n \cdot (\rho \vec{V} Y_{O_2}) \tag{14}$$

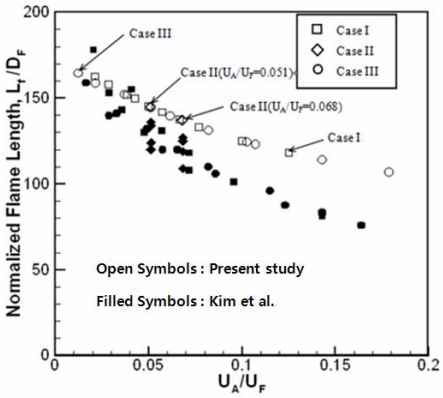

Fig. 3. Comparisons of predicted and measured flame lengths (nondimensionalized) in coaxial air flames vs. the ratio of coaxial air to fuel velocity. Open symbols: present study, filled symbols: Kim et al. [7].

$$\dot{m}_{O_2,DIFF} = \delta n \cdot (\rho D \nabla Y_{O_2}) \quad (15)$$

where $\dot{m}_{O_2,CONV}$ and $\dot{m}_{O_2,DIFF}$ are convective and diffusive mass fluxes per unit area, respectively. $\vec{V}$ and D are velocity vector and diffusion coefficient at the stoichiometric surface, δn is a unit vector normal to the stoichiometric surface, and symbol $\cdot$ denotes inner product.

Fig. 4 shows the changes of convective and diffusive fluxes of Y_{O_2} by coaxial air along the downstream direction. Two mixing modes both are augmented as coaxial air velocity rises, but the increased amount of convective flux is much less than that of diffusive flux. It implies that mixing enhancement mainly results from the increase of diffusive mixing augmentation rather than convective one, and that coaxial air increases substantially the effect of turbulent Reynolds stress involved in the diffusive flux. This fact can be elucidated by investigating Peclet number defined as Eq. (16) where the ratio of convective to diffusive effects is often used to measure the relative dominance of two mixing modes. In simple jet flames of Fig. 5(a), Peclet number remains constant regardless of fuel velocities and nozzle diameters at a given point. In contrast, in coaxial air flames of Fig. 5(b), Peclet number is shifted according as coaxial air velocity increases.

$$Pe_{,O_2} = \dot{m}_{O_2,CONV} / \dot{m}_{O_2,DIFF} \quad (16)$$

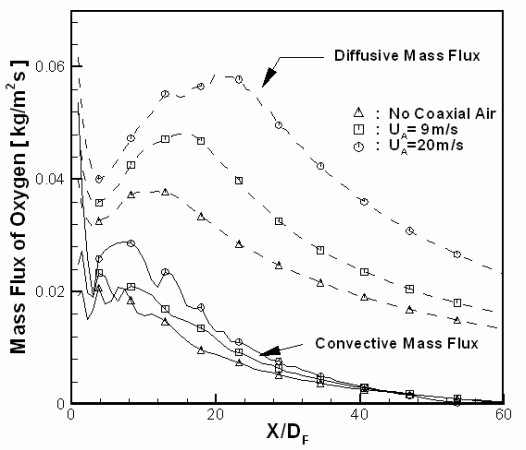

Fig. 4. The variation of convective (solid line) and diffusive (dashed line) mass fluxes of oxygen passing into stoichiometric surface with respect to different coaxial air velocities. U_F=244m/s.

At first, it was anticipated that a large amount of coaxial air entrained near fuel nozzle might penetrate into the flame reaction zone through flow convection. However, contrary to our expectations, the increase of oxygen supply into flames through flow convection was not important as U_A increased. This can be seen in Fig. 6 which shows the comparison of streamlines between simple jet flames and coaxial air flames. In the case of $U_A = 20m/s$ in Fig. 6(a), the air initially entrained toward the flame due to coaxial effect starts

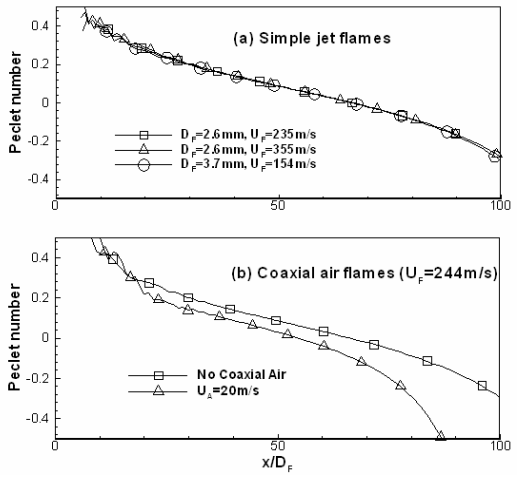

Fig. 5. The distribution of Peclet number at stoichiometric surface along the centerline. (a), simple jet flames; (b), coaxial air flames (U_F=244m/s). Note that Peclet number is changed by coaxial air, unlike simple jet flames.

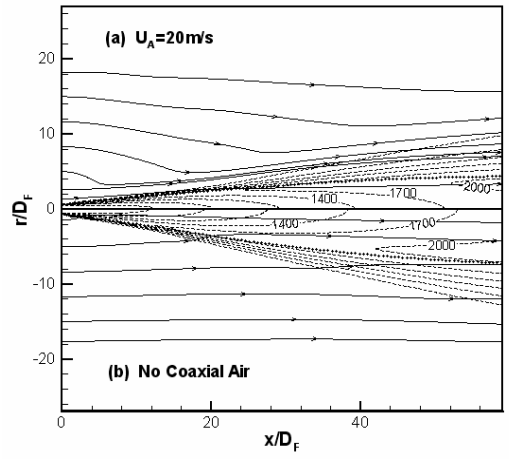

Fig. 6. The comparison of streamlines and temperature distribution of coaxial air flames to simple jet flames (a) coaxial air at U_A=20m/s, (b) no coaxial air, thin dashed line represents temperature contours, whereas solid line represents streamlines.

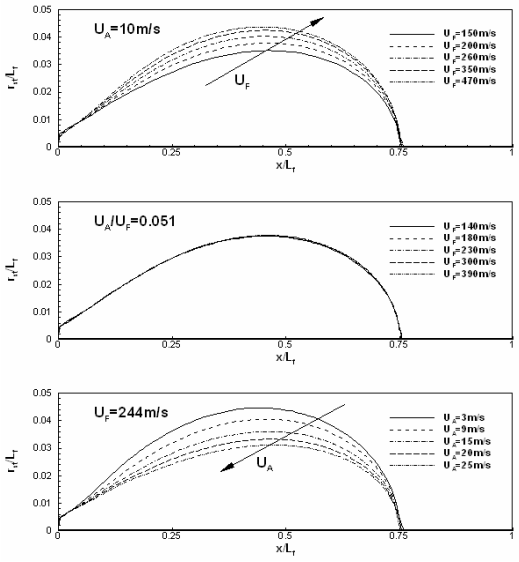

Fig. 7. The variation of flame shapes normalized by each flame length. (a), Case I (U_A=10m/s); (b), Case II (U_A/U_F= 0.051); (C), Case III (U_F=244m/s).

to ascend along high temperature zone, when reaching the reacting region. In contrast, in the case of no coaxial air in Fig. 6(b), the air initially following the coflow is easily entrained into the reacting region, as approaching high temperature zone. In other words, air is entrained toward high temperature zone at a higher angle in simple jet flames than in coaxial air flames, so that the increase of convective flux has a minor effect on the mixing augmentation of coaxial air. Thus, the effect of diffusive flux is believed to enhance the mixing mechanism significantly near the reaction zone, because the diffusive mass flux shown in Fig. 4 increases at a higher rate than convective flux as coaxial air velocity increases.

3.4 Flame self-similarity law

Simple jet flames are self-similar, which implies that mixture fraction distributions in each flame are identical when expressed in the nondimensional coordinates. The self-similarity of flames makes it possible for EINOx to be scaled with regard to different nozzle diameters, and for flame residence time to be simply defined with a flame length instead of a flame volume V_f because of two linear relations: $D_F \propto L_f$ and $V_f \propto L_f^3$. However, in coaxial air flames, the first relation does not hold in coaxial air flames, since coaxial air reduces the flame length as shown in Fig. 3, with the fuel nozzle fixed. Thus, we are interested in the validity of the second relation for EINOx scaling in coaxial air flames.

Flame shapes defined by the stoichiometric line are plotted in Fig. 7, after being normalized by their own flame length. In the case I (U_A=10m/s) of Fig. 7(a), normalized flame shapes become thicker as U_F increases from 150m/s to 470m/s, because the flame width increases at a faster rate than the flame length. In contrast, in the case III (U_F=244m/s) of Fig. 7(c), normalized flame shapes become thinner as U_A increases from 3m/s to 25m/s, since the flame width decreases at a faster rate that the flame length. And finally, in the case II (U_A/U_F=0.051) of Fig. 7(b) where the ratio of coaxial air to fuel velocity keeps a constant value, all normalized flame shapes collapse to a single line like in simple jet flames. As a whole, coaxial air flames have a tendency for their nondimensional flame shapes to be thinner as the ratio of coaxial air to fuel velocity increases. It implies that coaxial air can break down the flame self-similarity law, since the change rate of flame width is not the same as that of flame length, and thus, the second relation is also invalid. Therefore, the flame residence time for EINOx scaling must be defined using a flame volume, but not a cubic of a flame length.

4. Conclusion

The effect of coaxial air on flame length and self-similarity law is numerically analyzed for a wide range of flow conditions realizable by varying coaxial air and/or fuel velocity. The numerical methods and models used in this study are first verified and analyzed in the case of turbulent hydrogen-air jet flames without coaxial air and then extended to more complex flows driven by coaxial air. Three types of turbulent combustion model which account for either the presumed PDF model or the Lagrangian model are tested. It was found that the model including the HO_2/H_2O_2 chemistry not only reproduces the EINOx 1/2 scaling but also predicts EINOx most correctly among the three models. The following conclusions are drawn from results of this study regarding the characteristics of flame length and self-similarity law.

The results of simple jet flames demonstrate that HO_2/H_2O_2 chemistry should be taken into account for a better prediction of EINOx and its 1/2-power scaling law, which implies that they are sensitively affected by chemical nonequilibrium effect controlled by the third-body recombination.

Coaxial air augments fuel-air mixing by changing the flow dynamics existing between the coflow stream and fuel stream, and it is found that the mixing in the vicinity of high temperature zone mainly results from the increase of diffusive mixing effects due to the addition of extra turbulent fluctuations. Mixing enhancement by the convective flux of coaxial air was relatively slight when compared with that by the diffusive flux, because air is entrained into high temperature zone at a lower angle as coaxial air is increased. This overall mixing enhancement substantially reduces the flame shape, and eventually, the lessened flame volume decreases NOx production.

The rate of change of flame width did not show the same rate as that of flame length when coaxial air was supplied except for the case when the ratio of coaxial air to fuel velocity was fixed. A violation of the self-similarity law of simple jet flames is then observed. Therefore, two linear relations, $D_F \propto L_f$ and $V_f \propto L_f^3$, which have been used to simplify EINOx scaling parameters in simple jet flames without coaxial flame may no longer valid in coaxial air flames.

Acknowledgment

This work was supported by the Korea Science and Engineering Foundation (KOSEF) through the National Research Lab. Program funded by the Ministry of Education, Science and Technology (No. ROA-2007-000-10034-0)

References

[1] R. H. Chen and J. F. Driscoll, *Twenty-Third Symposium (International) on Combustion*, The Combustion Institute, (1990) 281-288.

[2] J. F. Driscoll, R. H. Chen and Y. Yoon, *Combust. Flame* (88) (1992) 37-49.

[3] J. Y. Chen and W. Kollmann, *Combust. Flame*, (88) (1992) 397-412.

[4] J. Y. Chen, W. C. Chang and M. Koszykowski, *Combust. Sci. and Tech.*, (1995) 505-529.

[5] M. Schlatter and J. C. Ferreira, *Twenty-Sixth Symposium (International) on Combustion*, Flury, M., and Gass, J., The Combustion Institute, (1996) 2215-2222.

[6] J. P. H. Sanders, J. Y. Chen and I. Gökalp, *Combust. Flame*, (111) (1997) 1-15.

[7] S.-H. Kim, Y. Yoon and I.-S. Jeung, Nitrogen Oxides Emissions in Turbulent Hydrogen Jet Nonpremixed Flames: Effects of Coaxial Air and Flame Radiation, *Proceedings of Combustion Institute*, (28) (2000).

[8] Y. Choi and C. L. Merkle, J. *Computational Physics*, (105) (1993) 207-223.

[9] J. Warnatz, U. Mass and R. W. Dibble, Combustion, *Springer-Verlag* Berlin Heidelberg, (1996) 67.

[10] G. Dixon-Lewis, F. A. Goldsworthy and J. B. Greenberg, *Proc. R. Soc. Lond. A.*, (346) (1975) 261-278.

[11] J. J. J. Louis, Turbulent Combustion of Coal Gas, *Ph. D. Dissertation*, U. of Twente, (1997).

[12] Siegel, Howell, *Thermal Radiation Heat Transfer*, McGraw Hill (1972).

[13] J. Villermaux, *Encyclopedia of Fluid Mechanics*, (1986) 707-768.

[14] R. S. Barlow and C. D. Carter, *Combust. Flame*, (104) (1996) 288-299.

[15] S. B. Pope, An Explanation of the Turbulent Round Jet/Plane Jet Anomaly, *AIAA Journal*, 16 (3) (1978) 279-281.

[16] W. J. A. Dahm and A. G. Mayman, *AIAA J.*, (28) (1990) 1157-1162.

[17] M. Kim, J. Oh, Y. Yoon and S. Kim, Length Scaling of Turbulent Hydrogen Nonpremixed Jet Flames with Coaxial Air, *32nd International Symposium on Combustion,* Montreal, (2008).

Hee-Jang Moon received his B.S. degree in Aeronautical Engineering from Inha University, Korea in 1986. He then received his M.S. and Doctoral degrees from Universite de Rouen, France in 1988 and 1991, respectively. Dr. Moon is currently a Professor at the School of Aerospace and Mechanical Engineering at Korea Aerospace University in Koyang, Korea. He serves on the Editorial Board of the Korean Society of Propulsion Engineers. His research interests are in the area of turbulent combustion, hybrid rocket combustion and nanofluids.